Immunity, Volume *56*

Supplemental information

Human microglia maturation is underpinned by specific gene regulatory networks

Claudia Z. Han, Rick Z. Li, Emily Hansen, Samantha Trescott, Bethany R. Fixsen, Celina T. Nguyen, Cristina M. Mora, Nathanael J. Spann, Hunter R. Bennett, Olivier Poirion, Justin Buchanan, Anna S. Warden, Bing Xia, Johannes C.M. Schlachetzki, Martina P. Pasillas, Sebastian Preissl, Allen Wang, Carolyn O'Connor, Shreya Shriram, Roy Kim, Danielle Schafer, Gabriela Ramirez, Jean Challacombe, Samuel A. Anavim, Avalon Johnson, Mihir Gupta, Ian A. Glass, Birth Defects Research Laboratory, Michael L. Levy, Sharona Ben Haim, David D. Gonda, Louise Laurent, Jennifer F. Hughes, David C. Page, Mathew Blurton-Jones, Christopher K. Glass, and Nicole G. Coufal

Supplemental Figure 1

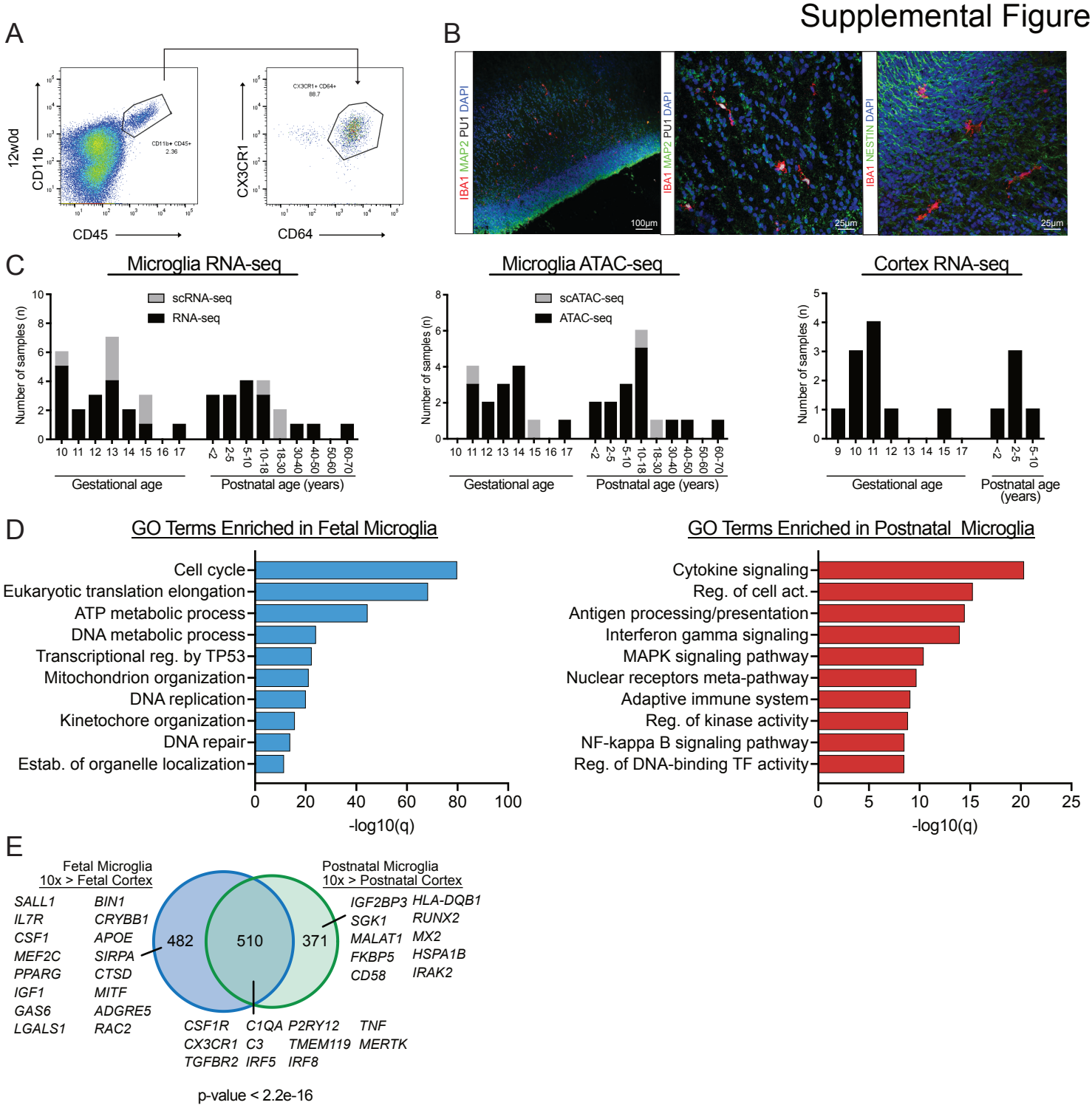

Figure S1 – Related to Figure 1. Transcriptomes of human fetal and postnatal microglia and brain tissue.

(A) Flow cytometry panel depicting sorting strategy for human fetal microglia. After live-dead and singlets gating, fetal microglia are defined by CD11b+CD45+CX3CR1+CD64+.

(B) Immunohistochemistry of 11w3d fetal brain illustrating colocalization of PU.1 (white) with IBA1 (red) positive cells and neurons, indicated by MAP2 staining (green). Microglia were identified throughout all brain regions.

(C) Bar charts depicting the number of samples per gestational week processed and analyzed for the indicated assays. Numbers for microglia are depicted in the left and middle panel while bulk fetal cortex is represented in the right panel. A fraction of the bulk RNA-seq, bulk ATAC-seq, and H3K27ac ChIP-seq data were curated from Gosselin et al., 2017 and Nott et al., 2019.

(D) Metascape enrichment analysis of differentially expressed genes between human fetal and postnatal microglia. Top enriched gene modules are shown, x-axis is the -log10(p) of the enrichment levels.

(E) Venn diagram illustrating overlap between genes enriched in fetal microglia as compared to fetal cortex (>10-fold, p-adj < 0.05 over bulk fetal cortex) and genes enriched in postnatal microglia compared to postnatal cortex. Important genes related to microglia function are listed.

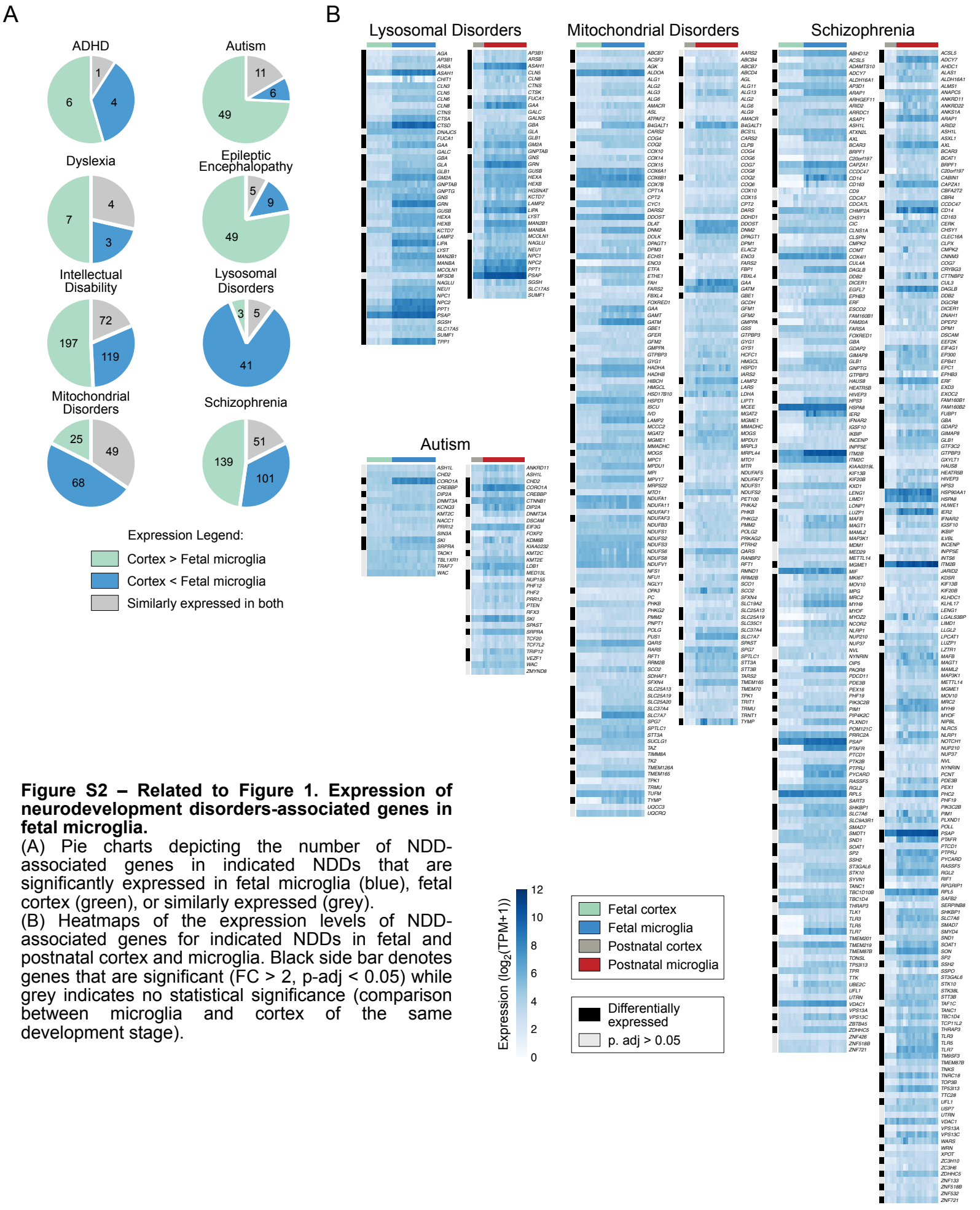

Figure S2 – Related to Figure 1. Expression of neurodevelopment disorders-associated genes in fetal microglia.

(A) Pie charts depicting the number of NDD-associated genes in indicated NDDs that are significantly expressed in fetal microglia (blue), fetal cortex (green), or similarly expressed (grey).

(B) Heatmaps of the expression levels of NDD-associated genes for indicated NDDs in fetal and postnatal cortex and microglia. Black side bar denotes genes that are significant (FC > 2, p-adj < 0.05) while grey indicates no statistical significance (comparison between microglia and cortex of the same development stage).

Fetal

Ligand	Cortical Cells
VCAM1	Radial glial cells
SEMA3F	Newborn excitatory neurons
DLL1	Radial glial cells
	Interneurons
	Intermediate progenitors of MGE
	Endothelial cells
	Astrocytes

Postnatal

Ligand	Cortical Cells
VIP	*VIP*+ GABAergic neurons
TGFB3	*LAMP5*+ GABAergic neurons
	LINC00507+ Glutamatergic neurons
	RORB+ Glutamatergic neurons
	FEZF2+ Glutamatergic neurons
BMP7	*FGFR3*+ Astrocytes
	RORB+ Glutamatergic neurons
	MYT1+ OPC
	LAMP5+ GABAergic neurons
VEGFA	*FGFR3*+ Astrocytes
	MYT1+ OPCs
	PVALB+ GABAergic neurons
IL6	*LINC00507*+ Glutamatergic neurons
	RORB+ Glutamatergic neurons
APOE	*FGFR3*+ Astrocytes
	MYT1+ OPCs
	LAMP5+ GABAergic neurons
CSF1	*OPALIN*+ Oligodendrocytes
	FGFR3+ Astrocytes

MGE - Medial ganglionic eminence
OPC - Oligodendrocyte progenitor cell

Figure S3 – Related to Figure 2. Putative cortical sources of ligands identified in NichNet. Putative cortical non-microglia cells expressing ligands identified in NicheNet analysis. Data derived from Allen Brain Map "Multiple Cortical Areas – SMART-seq (2019) dataset (https://portal.brain-map.org/atlases-and-data/rnaseq) and Nowakowski et al., 2017.

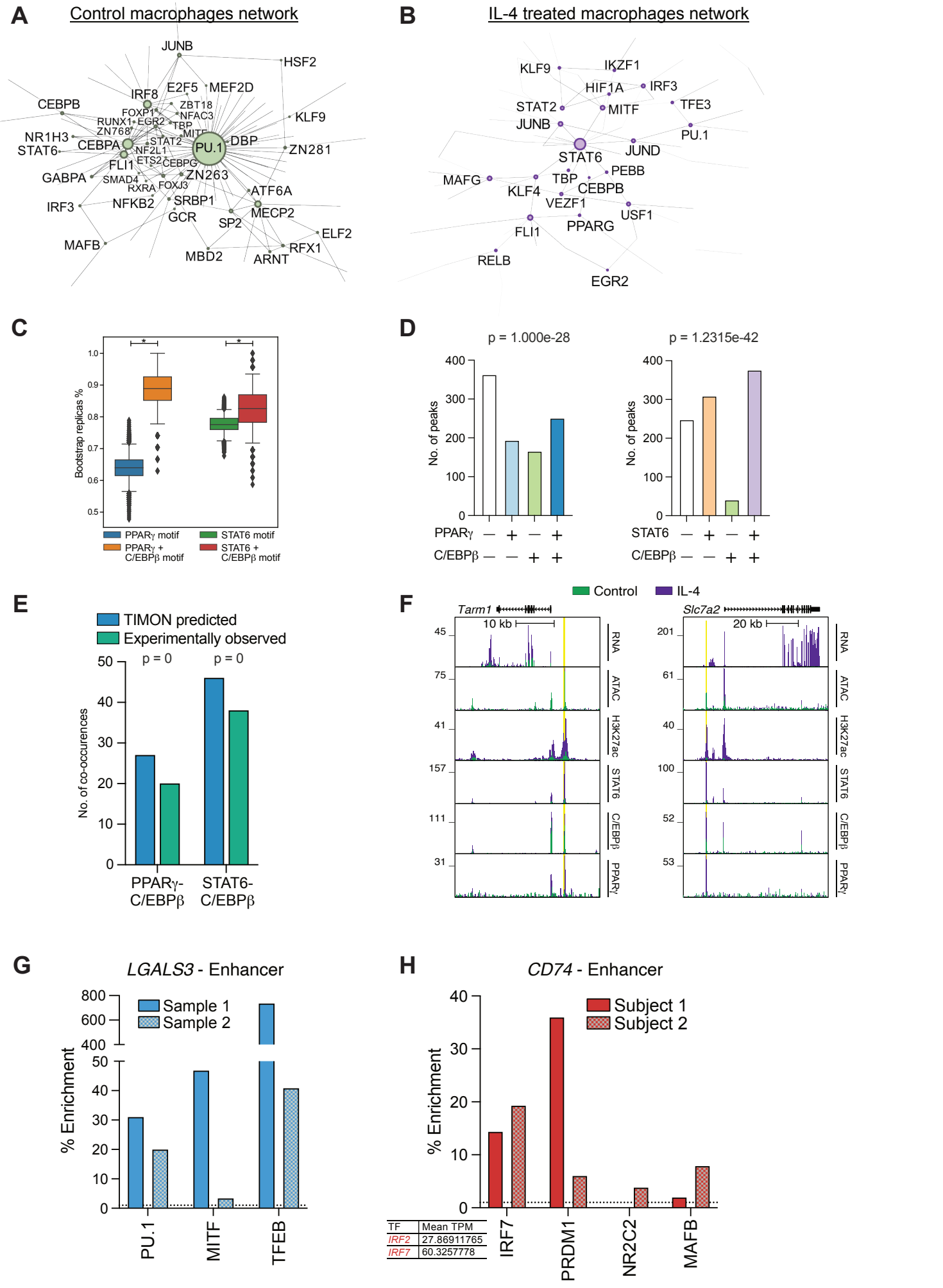
A
Control macrophages network
JUNB
HSF2
E2F5
MEF2D
IRF8
ZBT18
CEBPB
FOXP1
NFAC3
KLF9
RUNX1
EGR2
TBP
ZN768
NR1H3
MITF
CEBPA
STAT2
DBP
STAT6
NF2L1
PU.1
ZN281
ETS2
FLI1
CEBPG
GABPA
SMAD4
ZN263
RXRA
FOXJ3
ATF6A
IRF3
NFKB2
SREBP1
GCR
MECP2
SP2
ELF2
MAFB
RFX1
MBD2
ARNT
B
IL-4 treated macrophages network
KLF9
IKZF1
HIF1A
IRF3
STAT2
MITF
TFE3
JUNB
PU.1
STAT6
JUND
MAFG
TBP
PEBB
KLF4
CEBPB
VEZF1
USF1
PPARG
FLI1
RELB
EGR2
C
Bootstrap replicas %
PPARγ motif
STAT6 motif
PPARγ + C/EBPβ motif
STAT6 + C/EBPβ motif
D
p = 1.000e-28
p = 1.2315e-42
No. of peaks
PPARγ
C/EBPβ
STAT6
E
TIMON predicted
Experimentally observed
p = 0
p = 0
No. of co-occurences
PPARγ-C/EBPβ
STAT6-C/EBPβ
F
Control
IL-4
Tarm1
10 kb
Slc7a2
20 kb
RNA
ATAC
H3K27ac
STAT6
C/EBPβ
PPARγ
G
LGALS3 - Enhancer
Sample 1
Sample 2
% Enrichment
PU.1
MITF
TFEB
H
CD74 - Enhancer
Subject 1
Subject 2
% Enrichment
IRF7
PRDM1
NR2C2
MAFB
TF | Mean TPM
IRF2 | 27.86911765
IRF7 | 60.3257778

Figure S4 – Related to Figure 4. TIMON captures transcription factor interactions.

(A) Enhancer motif co-occurrence network (TIMON) of control BMDMs.

(B) The enhancer motif co-occurrence network unique to IL-4 treated BMDMs as predicted by TIMON. Each node represents a transcription factor motif, each edge represents significant ($p<0.001$) co-occurrence between two transcription factors.

(C) Significance test using bootstrap resampling procedure showing significantly increased PPARγ ChIP binding when the PPARγ motif occurs with the C/EBPβ motif (orange, mean=0.890) comparing with the PPARγ motif only (blue, 95% CI=0.565, 0.714). Same procedure was repeated for STAT6; when the STAT6 motif co-occurs with C/EBPβ, we observe a significantly increased chance of STAT6 TF ChIP binding (red, mean=0.826) compared with when only the STAT6 motif is present (green, CI=0.724,0.822).

(D) (left) Numbers of IL4 specific enhancers with both C/EBPβ and PPARγ, C/EBPβ or PPARγ and no C/EBPβ nor PPARγ transcription factor ChIP peak overlaps. Chi-square test was used to compute the p-value. (right) As with (left) but for transcription factor C/EBPβ and STAT6.

(E) Bar chart depicting the number of predicted peaks in which the indicated TFs co-bind (blue) and the number of the predicted peaks that were experimentally validated by TF ChIP-seq (green). Chi-square test was used to compute the p-value.

(F) UCSC genome browser RNA, ATAC-seq, and H3K27ac tracks of *Tarm1* (left) and *Slc7a2* (right) in control (green) and IL-4 treated (purple) BMDMs. Additionally, tracks showing STAT6, C/EBPβ, and PPARγ binding are also shown with yellow highlight indicating region in which TIMON predicted those TFs binding.

(G) ChIP-qPCR to analyze for fold enrichment of PU.1, MITF or TFEB at indicated *LGALS3*-associated enhancer (Figure 4F).

(H) ChIP-qPCR to analyze for fold enrichment of IRF7, NR2C2, PRDM1, and MAFB at indicated *CD74*-associated enhancer (Figure 4G). (lower right) Table showing mean TPM of *IRF2* and *IRF7* in postnatal microglia.

Supplemental Figure 5

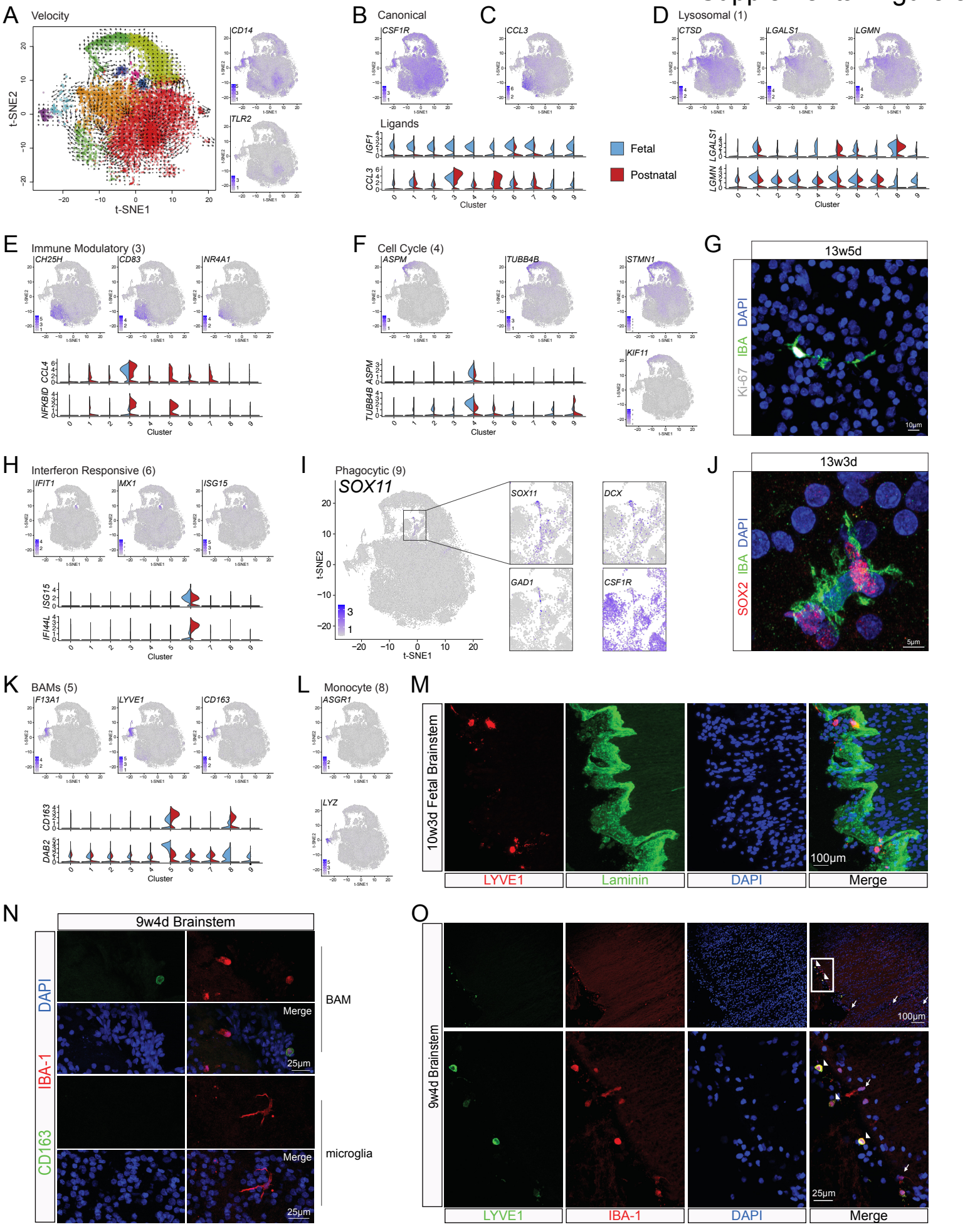

Figure S5 – Related to Figure 5. Cluster analysis of scRNA-seq of human fetal and postnatal microglia.

(A) RNA velocity analysis on scRNA-seq of fetal and adult microglia (left) and tSNE projection of relative expression for indicated genes (right).

(B) tSNE plot of expression of canonical microglia genes, *CSF1R.*

(C) (top) tSNE plot of *CCL3* expression. (bottom) Violin plots depicting log transformed expression of ligands, *IGF1* and *CCL3*, across clusters.

(D) Expression of genes enriched in the lysosomal cluster (cluster 1) from scRNA-seq data of human fetal and postnatal microglia, as projected onto tSNE plots or as log transformed values in violin plots across clusters.

(E) Expression of genes enriched in the immune modulatory cluster (cluster 3) from scRNA-seq data of human fetal and postnatal microglia, as projected onto tSNE plots or as log transformed values in violin plots across clusters.

(F) Expression of genes enriched in the cell cycle (cluster 4) from scRNA-seq data of human fetal and postnatal microglia, as projected onto tSNE plots or as log transformed values in violin plots across clusters.

(G) Immunohistochemistry of fetal microglia for Ki-67 as a marker of cell division.

(H) tSNE plots of relative expression of genes enriched in interferon responsive group (cluster 6) and violin plots of log transformed expression of select genes.

(I) tSNE plots of relative expression of genes enriched in phagocytic group that are associated with neural progenitor cells (cluster 9) and violin plots of log transformed expression of select genes.

(J) Immunohistochemistry of IBA1+ (green) fetal microglia engulfing a NPC, marked by SOX2 (red) staining.

(K) tSNE plots of relative expression of genes enriched in border-associated macrophage (BAM) group (cluster 5) Violin plot depicting log transformed expression of select cluster marker genes across clusters.

(L) tSNE plots of expression of genes in the monocyte cluster (8).

(M) Immunohistochemistry of fetal brain tissue showing colocalization of LYVE1 positive cells with the tissue border, detected by Laminin staining.

(N) Immunohistochemistry of fetal brainstem for border-associated macrophages (top), using CD163 and IBA1, juxtaposed by ramified microglia (bottom) that are CD163 negative.

(O) Immunohistochemistry of fetal brainstem for border-associated macrophages, using LYVE1 and IBA1.

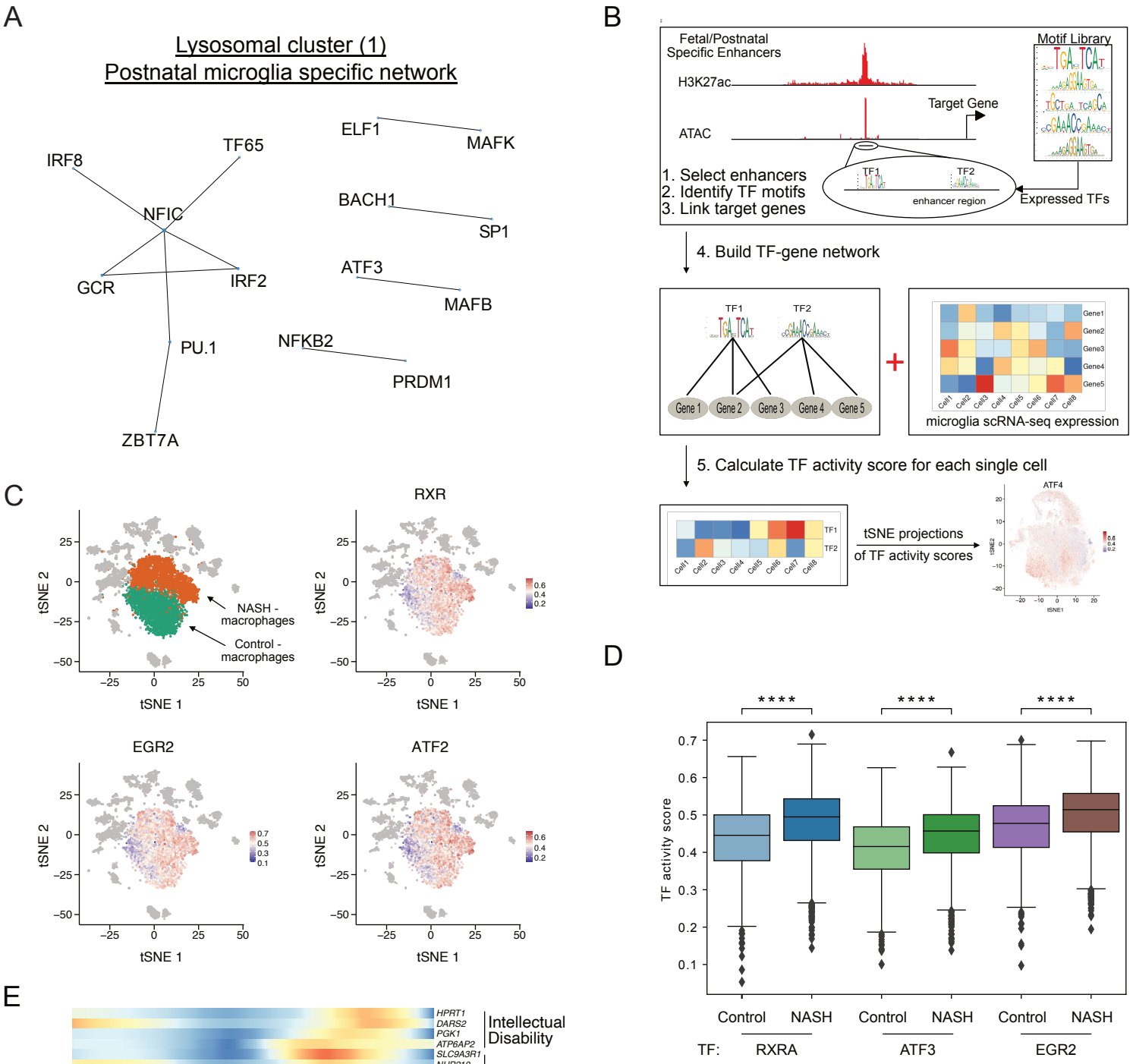

Supplemental Figure 6 – Related to Figure 5 and 6. Strategy for enhancer associated transcription factor activity (TFAct) and expanded by cluster TF activity analysis.

(A) Postnatal microglia specific TIMON analysis for cluster 1.

(B) Schematic of workflow for TFAct.

(C) tSNE projection of scRNA-seq of liver macrophages in control and NASH conditions (top left). Remaining are tSNE projections of TF activity scores for indicated TFs.

(D) Bar chart showing TF activity score in liver macrophages in control and NASH conditions as computed by TFAct. **** p<0.0001

(E) Heatmap showing genes associated with indicated neurodevelopmental disorders and their expression in primary human microglia and model systems.

Supplemental Figure 7

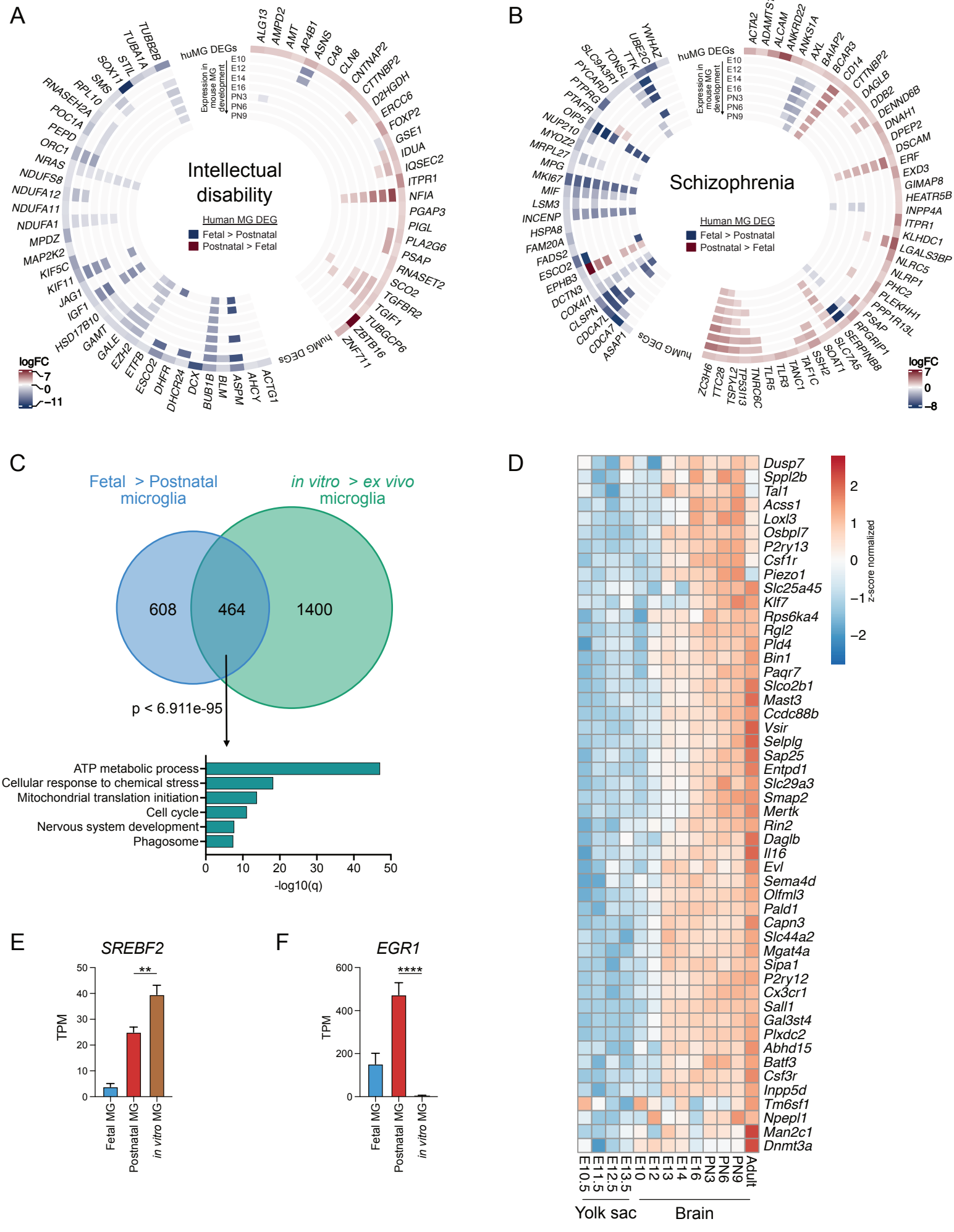

Supplemental Figure 7 – related to Figure 6 and 7. Environmentally regulated microglial genes share components with early fetal development.

(A.,B) Circos plot of genes associated with intellectual disability (A) and schizophrenia (B) that are differentially expressed in human fetal (blue) compared to postnatal microglia (red) (outer most track). Each inner track shows the status of these genes' ortholog in mouse differential expression analysis, where blue is higher expressed in the mouse microglia of the specified age compared to adult mouse microglia (red). Mouse ages progress as follows (outer to inner: E10.5, E12.5, E14, E16.5, PN3, PN6, and PN9). Grey denotes gene expression is nonsignificant between the indicated mouse microglia age and adult mouse microglia. PN: postnatal.

(C) Venn diagram showing overlap of human microglia developmental genes with genes that are environmentally regulated (top). (bottom) GO term analysis of genes indicated in overlap.

(D) Heatmap of one-to-one orthologous genes (mouse to human) that are part of the human microglia signature (fetal and postnatal) and are also changed when microglia are placed in culture.

(E) Bar chart showing expression of *SREBF2* (protein: SREBP2) in *ex vivo* human microglia and *in vitro* microglia.

(F) Bar chart showing expression of *EGR1* in *ex vivo* human microglia and *in vitro* microglia.

*p<0.05, ** p<0.01, *** p <0.001, **** p<0.0001